Journal of Constructional Steel Research 133 (2017) 167–180

Contents lists available at ScienceDirect

Journal of Constructional Steel Research

Experimental investigation on the seismic isolation for a legged wine storage tank

J.I. Colombo *, J.L. Almazán

Department of Structural and Geotechnical Engineering, Pontificia Universidad Católica de Chile, Vicuña Mackenna 4860, Santiago, Chile

ARTICLE INFO

Article history:
Received 16 August 2016
Received in revised form 29 January 2017
Accepted 11 February 2017
Available online xxxx

Keywords:
Wine storage tanks
Seismic isolation
Shaking table test
Compression springs

ABSTRACT

Because of the booming of the winery industry in some seismic countries such as, the U.S, Italy, Chile and Argentina, the seismic protection of wine storage tanks may be of a practical importance. Previous numerical and theoretical investigations have shown that seismic isolation can reduce the seismic demand on liquid storage tanks compared to the fixed base case. However, there are not experimental works about the seismic performance and protection of legged wine storage tanks, nor practical applications, reported in the technical literature. Therefore, in this paper, the effectiveness of a novel seismic isolation system has been investigated by shaking table tests on a full-scale legged tank, typically used in the wine industry. A comparison of the seismic behaviour of fixed base and isolated base configurations is presented. Two alternative base isolation systems have been studied: flat sliding bearings with a central leg acting as restoring element, and flat sliding bearings without any restoring element. The restoring force of the central leg was performed by means of five compression springs. The experiments were carried out using 3 natural and 3 artificial records. Measurements were made of the shear and axial forces in one leg of the tank, and the horizontal displacement of the tank. The experiments showed the beneficial effects of using the proposed isolation system in legged wine storage tanks, reducing the shear and axial forces in comparison with the fixed base configuration and reducing the horizontal displacement compared to the flat sliding bearing configuration without any restoring element.

1. Introduction

Stainless steel tanks are used in the winery industry for fermentation and storage since the 1950s in USA [1], and since the 1980s, approximately, in Chile and Argentina [2]. The use of this material, i.e. stainless steel, over other material for fermentation and wine storage tanks is due to its: (i) ease cleaning; (ii) noble chemical inertness; (iii) better control of the fermentation process; and (iv) aesthetically attractive appearance. However, several earthquakes have affected many of these tanks. For instance, many reports of damage provide evidence of failure and extensive damage in wine storage tanks such as during the 1977 Caucete earthquake in Argentina [3], the 1980 Livermore earthquake [4], the 1983 Coalinga earthquake [5], the 1989 Loma Prieta earthquake [6] and the 2003 San Simeon earthquake [7] (all in California, USA), the 2007 Pisco earthquake in Peru [2], the 2010 Maule earthquake in Chile [2], and the 2014 South Napa earthquake again in California, USA [8]. Therefore, the seismic vulnerability of these structures is evident.

The poor seismic reliability of wine storage tanks has caused considerable economic losses and environmental hazards by the loss of contents of these tanks [2]. The most common types of damage observed in liquid storage tanks are: damage to the piping connections caused by large base uplifts, damage to the roof caused by the sloshing of the free liquid surface, buckling of the tank walls caused by the high compressive stress, buckling of the tank legs caused by large axial loads coupled with lateral loads, failure of the anchorage system caused by the high overturning moment transmitted to the base, penetration of the tank wall with anchor bolts caused by the previous failure of the anchorage system and damage to the shell-base connection caused by the plastic rotation of the base plate. Among these causes, the failures that are responsible for a large or total loss of the liquids contained in storage tanks are buckling of the tank legs and rupture of the shell-base connection (see Fig. 1).

Stainless steel wine storage tanks are classified in two major groups: continuously supported tanks and legged tanks (see Fig. 2). Several damages have been reported for both types of tanks. For instance, in the past 2010 earthquake in Chile the losses reached approximately 125 million l of wine (250 million U.S. dollars) representing 12.5% of production in 2009 [2]. The earthquake struck a week before the start of the harvest, when only 50% of storage capacity was in use. This indicates that more than 25% of tanks with wine lost all or part of their content.

On the basis of the above-mentioned observations, and due to the successful of the wine industry in some seismic countries such as the

* Corresponding author.
E-mail address: jicolombo@uc.cl (J.I. Colombo).

http://dx.doi.org/10.1016/j.jcsr.2017.02.013
0143-974X/

Fig. 1. Typical failures in steel wine storage tanks that imply loss of the liquid content: (a) buckling of the tank legs and (b) rupture of the shell-base connection.

US, Italy, New Zealand, Chile and Argentina among others, seismic protection of wine storage tanks in the face of earthquake hazards is of paramount economic importance.

Recently numerous studies have been carried out in this field in order to improve seismic behaviour and to reduce the risk of damage or failure of liquid storage tanks [9,10]. In these studies two major alternatives are presented: seismic isolation and external energy dissipation. Some examples of seismic protection in liquid storage tanks using isolation systems are given by Shrimali and Jangid [11], Cho et al. [12], and Almazán et al. [13]. Similarly, examples of seismic protection in liquid storage tanks using external energy dissipation devices are published by Maleki and Ziyaefar [14,15], Pirner and Urushadze [16], Liu and Lin [17], Malhotra [18], Curadelli [19], Ormeño et al. [20] and Colombo and Almazán [21]. However, only a few works have been found in the technical literature concerning the seismic performance and protection of legged tanks. For instance, Almazán et al. [13] investigated numerically the seismic response of a typical wine legged tank with seismic isolation in the bottom of its legs. Nevertheless, to the best of the author's knowledge, any experimental investigation about the seismic performance and protection of legged tanks has been reported in the technical literature.

Therefore, in this work the effectiveness of a novel isolation system on a legged wine storage tank has been investigated through shaking table test on full-scale of a real tank, typically used in the wine industry for fermenting and storing relatively small volumes of high quality wines. More precisely, with the purpose of evaluating the effectiveness of using a novel seismic isolation system in this structure, the seismic response of this tank with the isolation system was compared to that of fixed-base configuration. The isolation system was consisted of one multi-spring central leg, acting as a restoring element (i.e. the element responsible for the self-centring capacity), and one flat sliding bearing below each tank leg. Three tank anchorage configurations were evaluated: fixed base, isolated base without the restoring element (i.e. just with the flat sliding bearings) and isolated base with the restoring element. The force-displacement relationship of the multi-spring central leg was numerically established by means of an ANSYS model and the respective pushover analysis. The tests, which have been performed at the Laboratory of the Department of Structural and Geotechnical Engineering of the Pontificia Universidad Católica de Chile, demonstrated the effectiveness of the herein proposed seismic protection system.

2. Wine-tank considered

Experimental tests were carried out on a full-scale stainless steel legged tank which is typically used for fermentation and wine storage (see Fig. 3). When subjected to a strong seismic ground motion the structure may undergo several failure modes. The most significant failure modes are: buckling of the tank legs and failure of the anchorage bolts at the legs. Therefore, the purpose of this research is to avoid such failures modes using a new device for seismic isolation.

The dimensions of the tank are: radius $R = 0.8$ m, wall height $H_w = 1.70$ m, and length of the legs $L_g = 0.9$ m. The wall, base and legs are realized with stainless steel plates having a thickness of 2 mm. The tank is supported on four legs with upper width $w_u = 22$ cm, and lower width

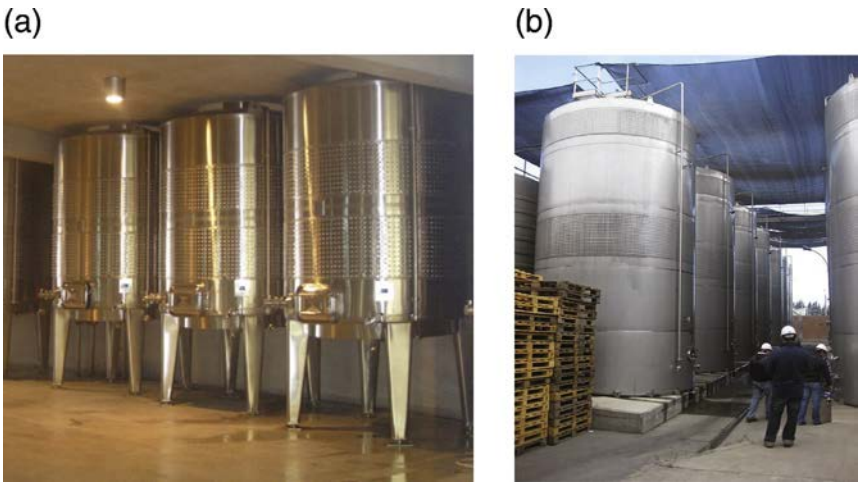

Fig. 2. Different foundation schemes for wine storage tanks: (a) legged tanks and (b) continuously supported tanks.

Fig. 3. Legged wine storage tank utilized in the experiments.

$w_l = 10$ cm. The liquid used in the experimental campaign is water, which has the same density of wine. The tank is completely filled due to the fact that these tanks are completely filled in the wine industry. The total mass of the liquid and the tank is about 3300 kg.

During the experimental campaign three different configurations were analysed (see Fig. 4). The first configuration was the tank without the isolation system, in which the tank was just anchored to the foundation. The second configuration was the tank with the isolation system (i.e. the multi-spring central leg and the flat sliding bearings). The third configuration was the tank isolated only with the flat sliding bearings (i.e. without the multi-spring central leg). In the configuration with the multi-spring central leg, this central leg was anchored to the tank base and the shaking table. Additionally, it important to remark that the multi-spring central leg did not receive weight load from the tank, i.e. the weight of the tank was resisted by the original tank legs.

3. Base-isolation system

The used of the base isolation technique is one of the most efficient mechanisms available for seismic protection. The first works of base isolation system to afford seismic protection to liquid storage tanks are attributed to Chalhoub and Kelly in 1988 [22]. Since then, several works on this subject have been presented (see e.g. [11–13]). Unfortunately, few practical applications have been implemented [23] and a limited number of experimental works have been carried out [24].

For this investigation, the isolation system consisted of one multi-spring central leg, responsible of the restoring force, and one flat sliding bearing below each tank leg (see Fig. 5). As mentioned above, the multi-spring central leg did not receive weight load from the tank, it just provided the restoring force. Due to the simplicity of the construction and the common use of spring as restoring element, compression springs were used for the central leg. Moreover, the springs used at the bottom and the top of the central leg acted as spherical ball joints as well, i.e. the pattern in which the springs were used allows the tank to move horizontally in any direction. In other words, the springs were used in a vertical arrangement due to: (1) the simplicity of construction of the central leg, and (2) in order to allow the tank to move horizontally in any direction but using the flexural, shear and axial stiffnesses of the compression springs (see Fig. 4(b)). The multi-spring central leg was made with five spring, two big square plates, two small square plates and one tube. The side length of the big plates and the small plates were 50 cm and 27 cm, respectively. The thicknesses of these plates were 1 cm. The dimensions of the tube were: internal diameter $\phi_i = 16$ cm, external diameter $\phi_e = 18$ cm, and length $l = 44.6$ cm. The dimensions of the springs were: free length $l_s = 13.7$ cm, wire diameter $d_w = 1.8$ cm, pitch $p = 3.7$ cm and external diameter $\phi_{es} = 16.2$ cm. The material of the springs was SAE 9254 steel. The central leg had the linear approximation for the lateral force-displacement relationship shown in Fig. 6. This relationship was obtained by the method described in the section below. The isolation period, calculated with the linear approximation of the lateral force-displacement and the total mass of the structure, was about of 2 s. In this context, it is worth mentioning that

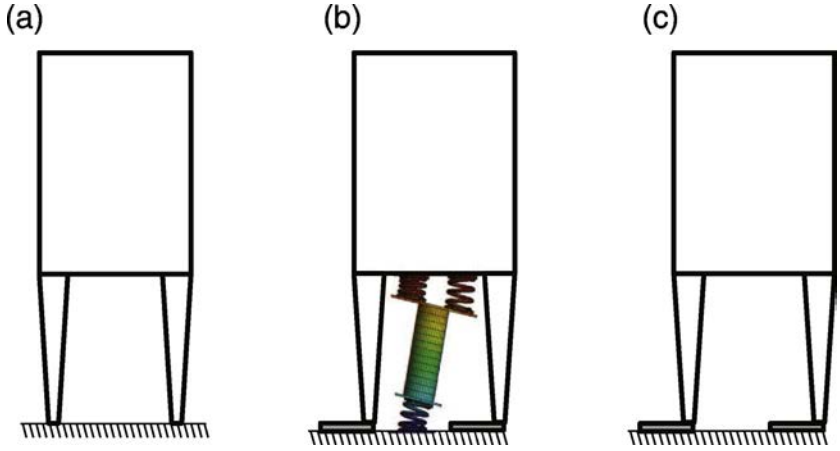

Fig. 4. Sketch of the three different configuration analysed during the experimental campaign: (a) fixed base configuration, (b) isolated with the multi-spring central leg and the flat sliding bearings and (c) isolated only with flat sliding bearings.

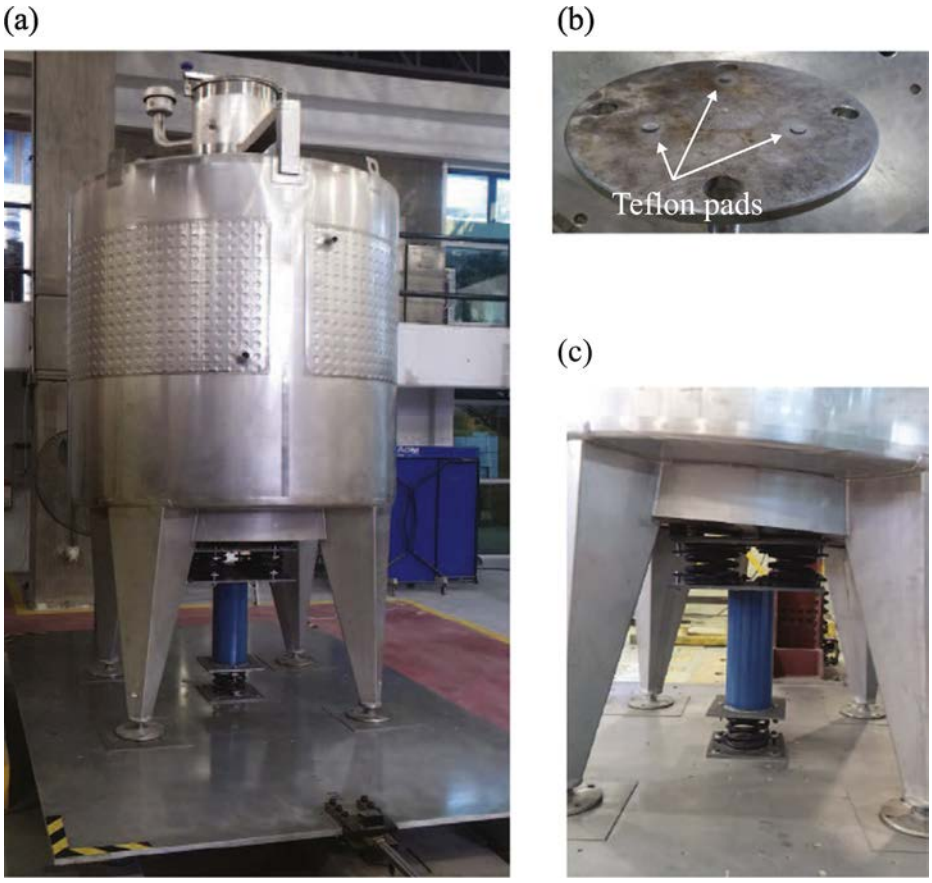

Fig. 5. Multi-spring central leg and flat sliding bearings installed on the legged wine storage tank: (a) general view, (b) Teflon pads and (c) the multi-spring central leg connected to the tank and the shaking table.

this is a novel approach to use these types of springs, i.e. using the flexural, shear and axial stiffnesses of compression springs. Some other options for realizing the restoring element can be: (a) an auxiliary structure connected to the roof of the tank, (b) a central-leg with a traditional rubber isolator on the top of the leg (Fig. 7).

With respect to the flat sliding bearings used in the proposed isolation system, four stainless steel plates of size 500 mm × 500 mm and thickness 2 mm were used. Each plate was placed below of each leg of the tank. Additionally, three Teflon pads were embedded on the bottom of each leg of the tank (see Fig. 5(b)). The diameter and length of each Teflon pads were 10 mm and 5 mm, respectively.

Additionally, it is also worth mentioning that legged wine storage tanks have usually a stiffener ring that connects the top of the legs with the base of the tanks. This stiffener ring is one of the robust parts of the tank, and is the most suitable place to connect the restoring element (see Fig. 8).

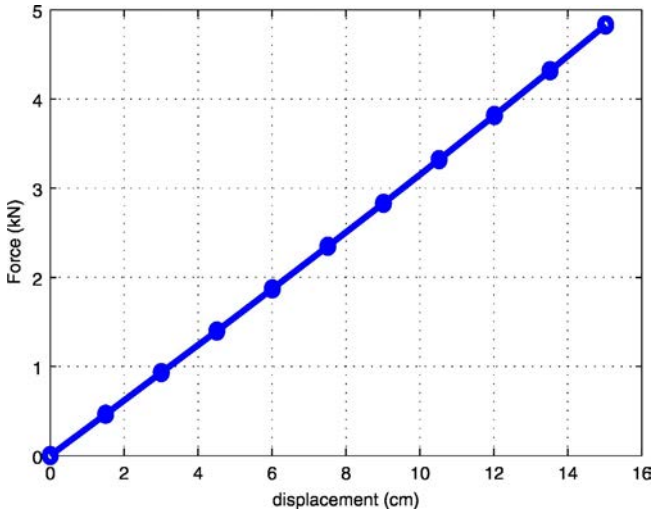

Fig. 6. Force-displacement relationship for the multi-spring central leg.

4. Multi-spring central leg model

In order to obtain the force-displacement relationship of the multi-spring central leg, and to ensure that the multi-spring central leg will work correctly without failure, a 3D finite element model was used. This model was developed in ANSYS, and the force-displacement relationship and stress verification were carried out with the aid of non-linear static pushover analysis. The stress-strain relation was determined by means of a bilinear isotropic hardening model, where the material parameters of the stress-strain relation for the plates and the tube were as follows: the Young modulus of elasticity and the yielding stress were 193 GPa and 310 MPa, respectively; the Poisson ratio was 0.3; and the tangent modulus was 1.8 GPa. However, the material used for the springs was SAE 9254 steel which had a Young modulus of elasticity of 205 GPa and a yielding stress of 1470 MPa. The device was discretized using a 3-D 20-node solid element exhibiting a quadratic displacement behaviour (SOLID186). This element has three degrees of freedom per node (i.e. translation in the x, y and z directions of the nodal) and makes it possible to perform a non-linear analysis. Large displacement and deformation effects, such as large deflection, large rotation and large strain, were accounted for by using the non-linear geometry option in ANSYS.

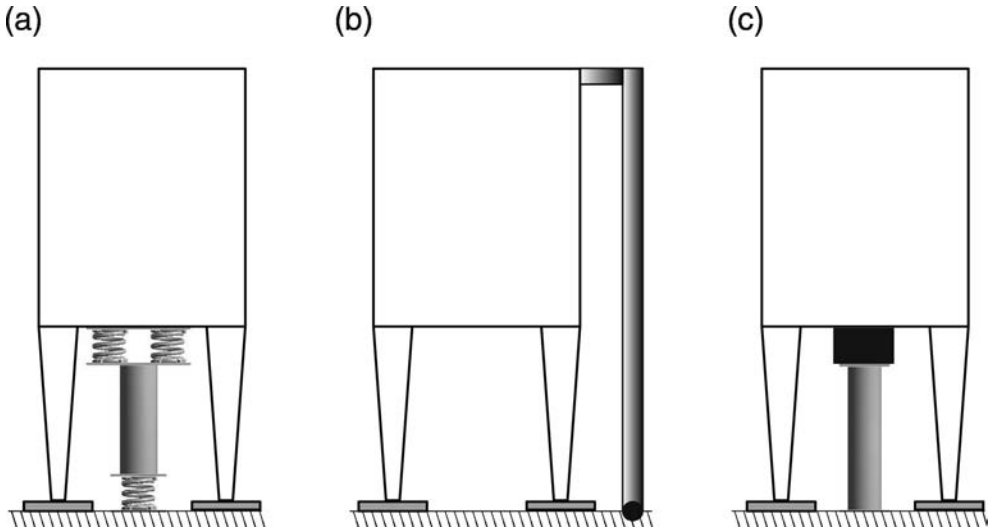

Fig. 7. Some possible options for realizing the restoring element: (a) a multi-spring central leg, (b) an auxiliary structure connected to the tank, and (c) a central leg with a traditional rubber isolator.

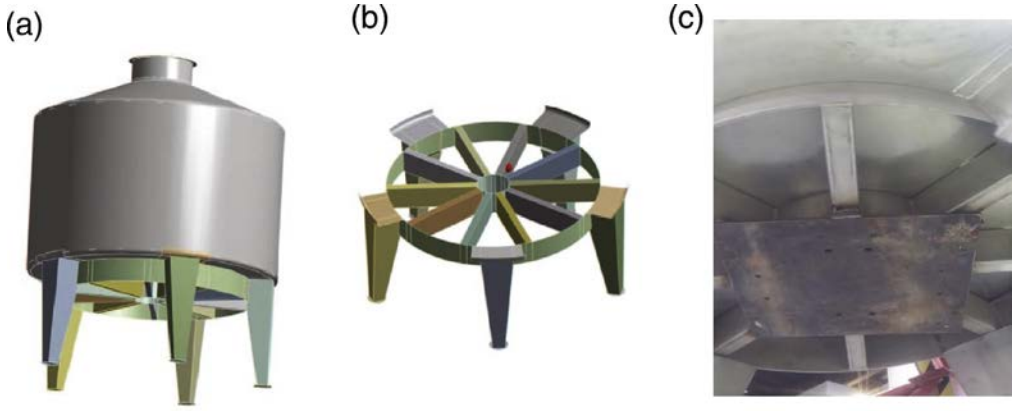

Fig. 8. The stiffener ring of a typical legged wine storage tank: (a) schematic views the entire tank and (b) the stiffener ring of the tank [2]; and (c) an image of the stiffener ring of the current tank with the welded plate where is connected the multi-spring central leg.

Horizontal rollers located above the top plate were used to simulate the surrounding tank structure. These rollers kept the top plate horizontal during the lateral displacement of the tank. The bottom plate was fixed to the foundation (see Fig. 9).

4.1. Stress verification of the multi-spring central leg

Non-linear static pushover analysis for the multi-spring central leg was carried out (displacement control analysis) using the multi-spring

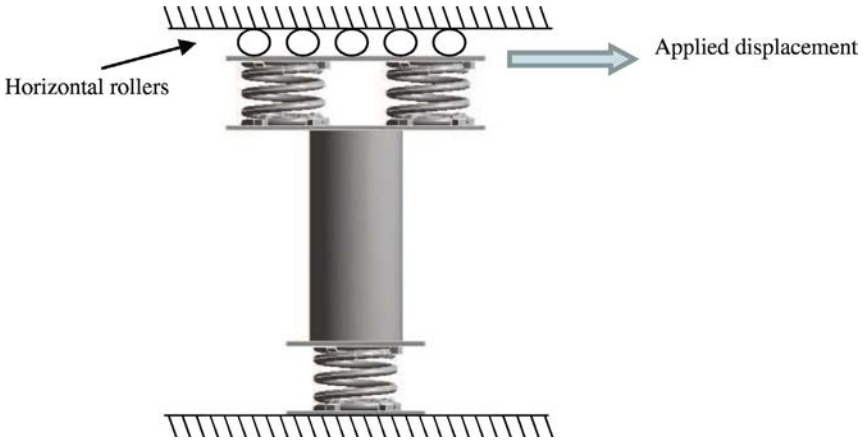

Fig. 9. Boundary conditions and applied loading on the multi-spring central leg model.

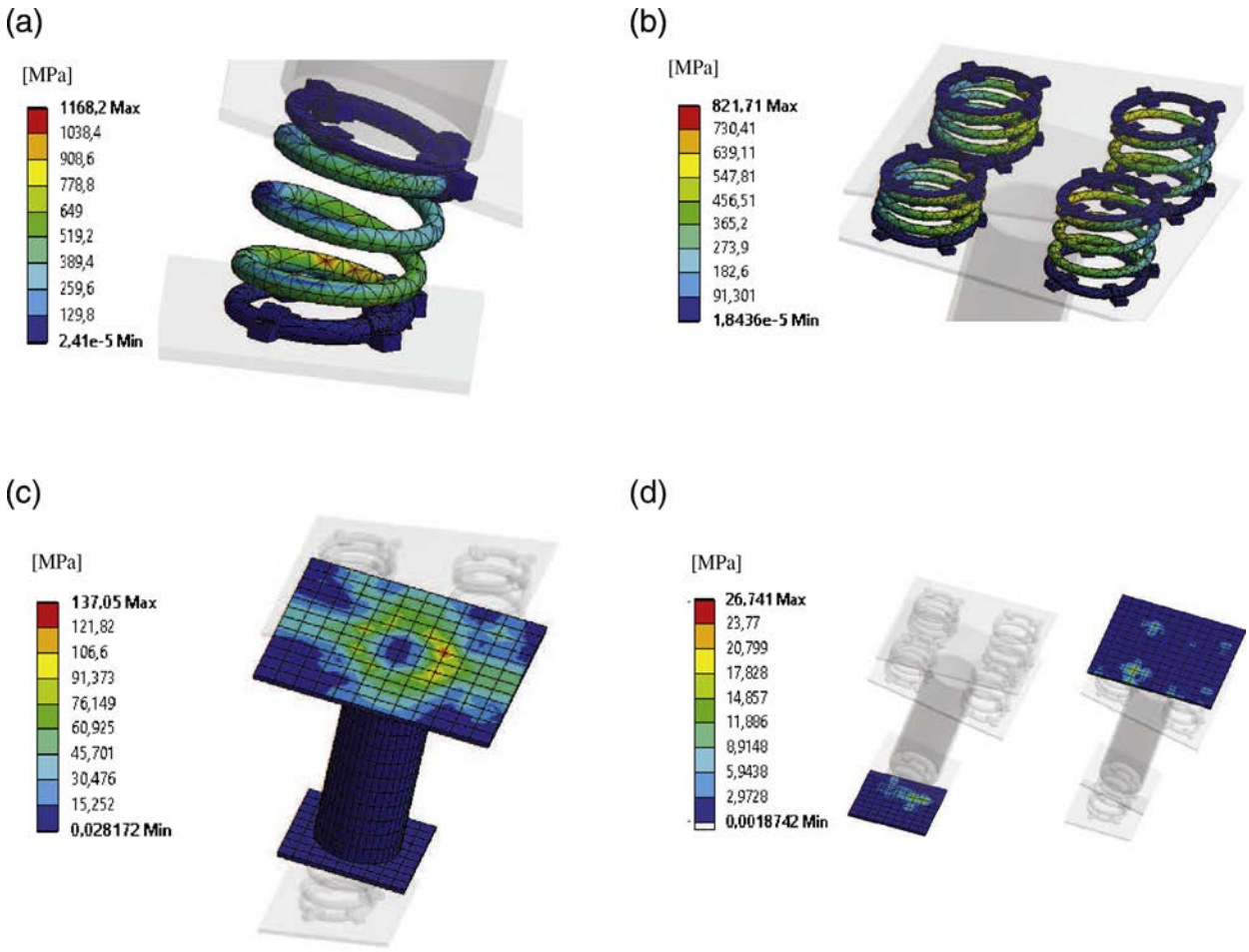

Fig. 10. Von Mises stress distribution (in MPa) of the model subjected to horizontal displacement applied to the top plate at maximum condition for: (a) the bottom spring; (b) the top springs; (c) the tube and centre plates; and (d) the top and bottom plates.

central leg model described above. Horizontal displacement history was applied to the top plate following a ramp-shaped function, i.e. linear and monotonic increasing. The horizontal displacement was raised up to 15 cm. This value was the maximum desirable displacement in order to maintain safety the compression springs. Nevertheless, in order to maintain the safety of the surrounding structures and piping connections, the maximum allowed displacement was of 10 cm. The displacement step was equal to 15 mm.

The Von Mises stress distribution of the structure subjected to horizontal displacement was calculated for each displacement step. The maximum Von Mises stress value in the springs was 1168 MPa (Fig. 10(a)). In the other parts of the central leg, i.e. the tube and the plates, the maximum Von Mises stress value was 137 MPa. In both cases, the structure is shown in the deformed configuration (Fig. 10). As expected, the stresses were highly concentrated at some coils of the springs, where the maximum effective stress reached 1168 MPa. Hence, comparing these maximum stress values with the yielding stresses indicated above, i.e. 310 MPa for steel of the plates and the tube and 1470 MPa for SAE 9254 steel used in the springs, it can be concluded that the multi-spring central leg will remain without failure. As mentioned above, the lateral force-displacement relationship of the central leg is shown in Fig. 6.

5. Test programme and sensor setup

A series of dynamic tests have been accomplished on the tank using the shaking table installed at the Laboratory of the Department of Structural and Geotechnical Engineering of the Pontificia Universidad Católica de Chile. During the experimental campaign the tank has been tested in three different configurations: isolated base with the multi-spring central leg and the flat sliding bearings (referred as case CL), isolated just with the flat sliding bearings (referred as case SB), and fixed to the shake table (referred as case FB).

A set of six different base motion histories have been utilized in each configuration. More precisely, the horizontal component of three natural (see Table 1) and three artificial records (ART1, ART2 and ART3), in accordance with the Chilean code spectrum for 5% damping and soil classified as type II [25], were scaled to different intensity levels. Due to the fact that the tested structure was on the real scale, no time scaling operation was necessary. All the records were filtered using a high-pass filter with a cut-off frequency of 0.1 Hz. The different intensity levels used for the natural and artificial records were: 100%, 120% and 150% for case CL (i.e. scale factor of 1, 1.2 and 1.5, respectively); 50%, 70%, 90% and 100% for case SB (i.e. scale factor of 0.5, 0.7, 0.9 and 1, respectively); and 30%, 40% and 50% for case FB (i.e. scale factor of 0.3, 0.4 and 0.5, respectively). The records selected are shown in Table 1, and their respective response spectra are shown in Fig. 11.

Table 1
Characteristics of the natural accelerograms used during the experimental campaign (recorded at M_w 8.8 2010 Maule, Chile Earthquake).

Accelerogram	PGA (g)	Duration (s)
Curicó	0.470	180
Hualañe	0.461	144
Talca	0.477	148

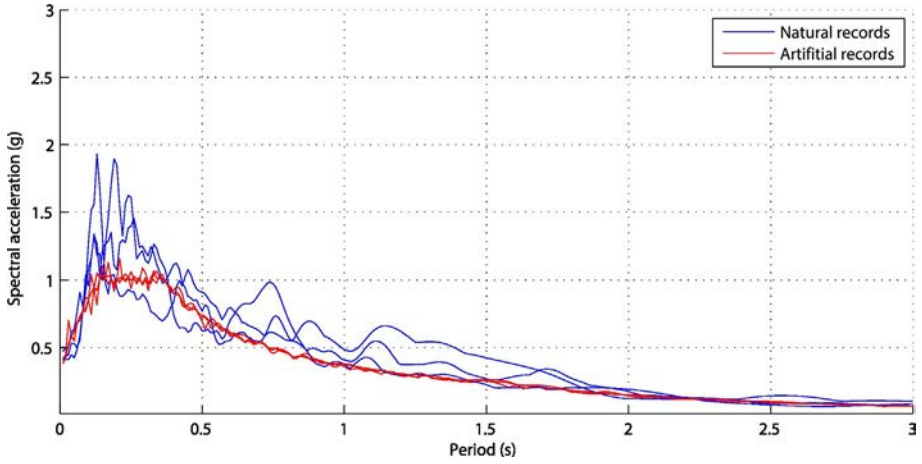

Fig. 11. Response spectra ($\xi = 5\%$) of the 3 natural and the 3 artificial records.

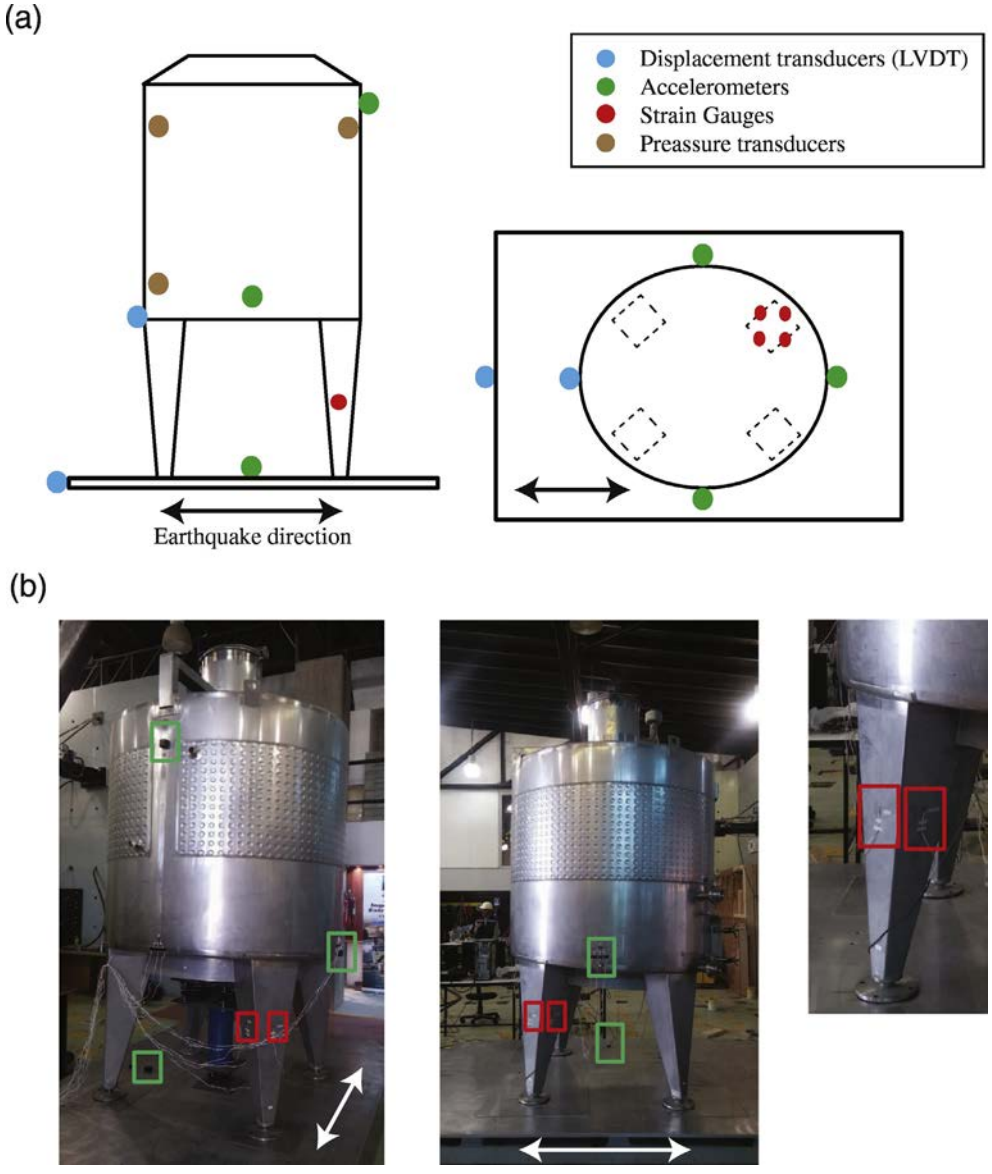

Fig. 12. Placement of sensors on the tank: (a) sketch of elevation and plant views; and (b) images of the tank with the sensors.

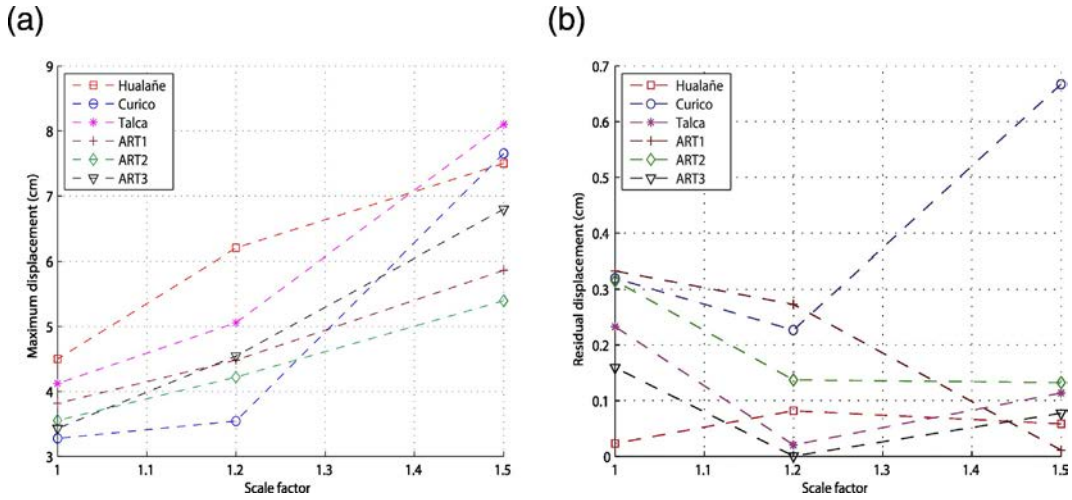

Fig. 13. (a) Maximum lateral displacement and (b) residual displacement of the tank versus scale factor for the six selected records in the case CL.

The sensor setup for the acquisition of the structural response consisted of: two LVDTs, four strain gauges, four accelerometers and three pressure transducers. The type and location of the sensors to test the isolated system are shown in Fig. 12. The two LVDTs were used to measure the displacement of the tank with respect to the shaking table in cases CL and SB. The four strain gauges were used to compute the axial and shear forces of one leg of the tank. Three of the four accelerometers were used to measure the wall tank horizontal acceleration, and the fourth accelerometer was used to measure the horizontal acceleration of the shaking table. All the accelerometers were orientated in the direction of the applied motion.

6. Analysis of results

The effectiveness of a novel isolation system on a legged wine storage tank has been assessed through shaking table test on full-scale of a real tank. The procedure for the shaking table test was described in Section 5.

6.1. Response of the base-isolated tank with the multi-spring central leg and the flat sliding bearings

The tank configuration using the multi-spring central leg and the flat sliding bearings (case CL) was seismically tested using the previous described set of six records. The tests were conducted by scaling each record, starting from an intensity of 100% and repeating the test with increasing intensity up to 150%. The results of the most significant quantities that were acquired during the tests are compared with the results obtained in the other tank configurations, i.e. cases SB and FB, in a later section (Section 6.4). In particular, we focus on the following quantities:

1) displacement of the tank relative to the shaking table
2) shear and axial forces at the tank leg
3) total shear

In particular, the shear and axial forces are ones of the most important quantities because the most common failure on legged tanks occurs when the combined effect of both forces provokes the buckling failure of the legs. The shear and axial forces can be easy calculated because of the elastic behaviour of the stainless steel using two pairs of strain gauges that are located at one of the tank legs (Fig. 12(b)).

The maximum lateral displacements and the residual displacements of the tank are compared for the used scale factors and records. Fig. 13(a) shows the maximum displacement of the tank for each records and scale factors. As expected, the maximum displacement increased with the rising of the scale factor for all the used records. The values of the maximum displacement varied from 3 cm and 5 cm, approximately, for a scale factor of 1, up to 5 cm and 8 cm, approximately, for a scale factor of 1.5. This maximum value of 8 cm does not provoke any failure at the multi-spring central leg (see Section 4.1), and seems to be a

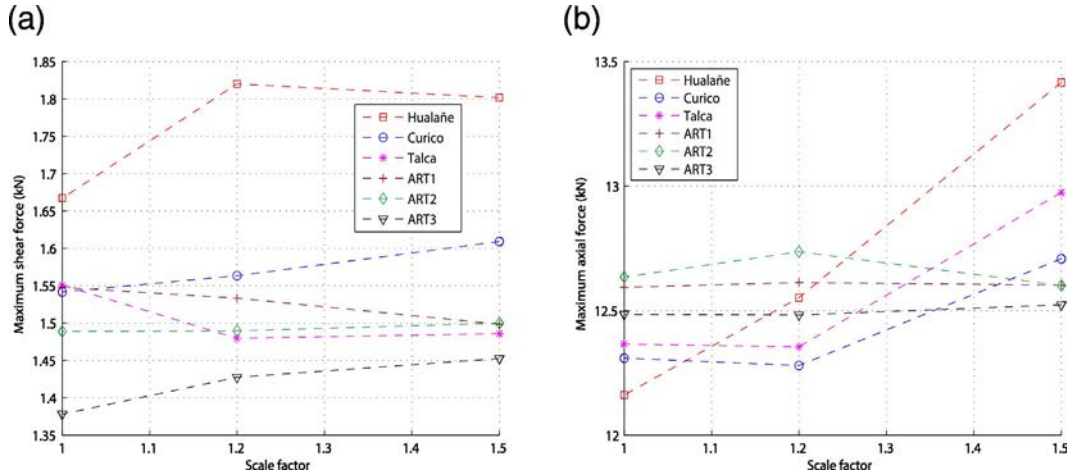

Fig. 14. Maximum values of (a) shear and (b) axial forces at the tank leg versus scale factor for the six selected records in the case CL.

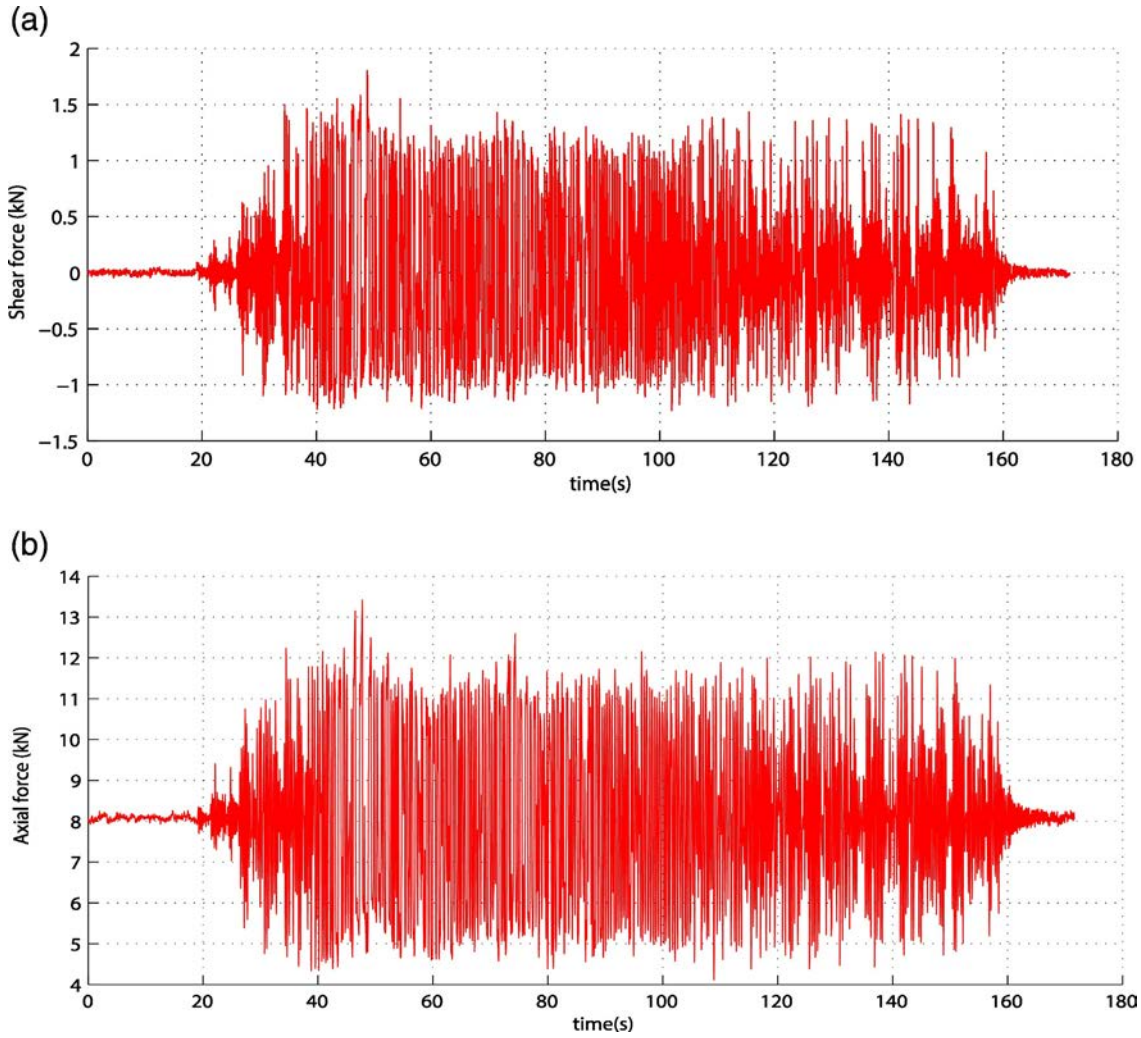

Fig. 15. (a) Shear and (b) axial forces because of Hualañe accelerogram with a scale factor of 1.5 in the case CL.

reasonable allowed displacement in order to maintain safety the piping connections and the surrounding structures. With respect to the residual displacement, Fig. 11(b) shows the residual displacement for each records and scale factors. All the values of the residual displacement are almost negligible (i.e. lower than 1 cm). These results show that the restoring force of the multi-spring central leg was quite effective for the analysed tank.

Fig. 14(a) and (b) show the maximum values of the shear and axial forces at the tank leg, respectively. The maximum shear force at the tank leg was bounded by the mobilized frictional force, and presented an average of 1.5 kN. In reference to the maximum axial force at the tank leg, it was also bounded to 12.8 kN (compression force), approximately. This bound was also consequence of the mobilized frictional force. More precisely, as the maximum total shear transmitted to the tank was bounded by the mobilized frictional force, the maximum overturning moment was bounded by this maximum total shear. Therefore, as the responsible of the dynamic increment on the axial force at the tank legs is the overturning moment, the maximum axial force was also bounded. The bounds on the maximum values of the shear and axial forces were also noticeable in the time history of all the tests. For brevity only the results of the Hualañe record, scaled with a scale factor of 1.5, are shown (Fig. 15).

Finally, in order to compare the numerical and experimental force-displacement relationship of the multi-spring central leg, a linear least square fitting was carried out for the total shear as a function of the tank displacement (see Fig. 16). As mentioned above, only the results of the Hualañe record with a scale factor of 1.5 are shown. The value of the experimental linear stiffness was 332 N/cm. This experimental value is very close to the value predicted by the model described in Section 4 (318 N/cm). Therefore, the force-displacement relationship of the multi-spring central leg has been validated numerically and experimentally.

In conclusion, the results presented herein show that the tank with the multi-spring central leg and the flat sliding bearings remained without failure for a scale factor up to 1.5. More precisely, the tank remained without failure for the six records scaled up to the maximum intensity level of 0.72 g of PGA.

6.2. Response of the base-isolated tank with the flat sliding bearings

Similarly to the section above, the tank configuration using the flat sliding bearings (case SB), i.e. without the multi-spring central leg, was seismically tested using the previous described set of six records. The tests were conducted by scaling each record, starting from an intensity of 50% and repeating the test with increasing intensity up to 100%.

Fig. 17 shows the maximum lateral displacements and the residual displacements of the tank for the used scale factors and records. As expected, the maximum displacement increased with the rising of the scale factor for all the used records (see Fig. 17(a)). The values of the maximum displacement varied from 2 cm and 5 cm, approximately, for a scale factor of 0.5, up to 6 cm and 17 cm, approximately, for a scale factor of 1. We consider that this maximum value of 17 cm

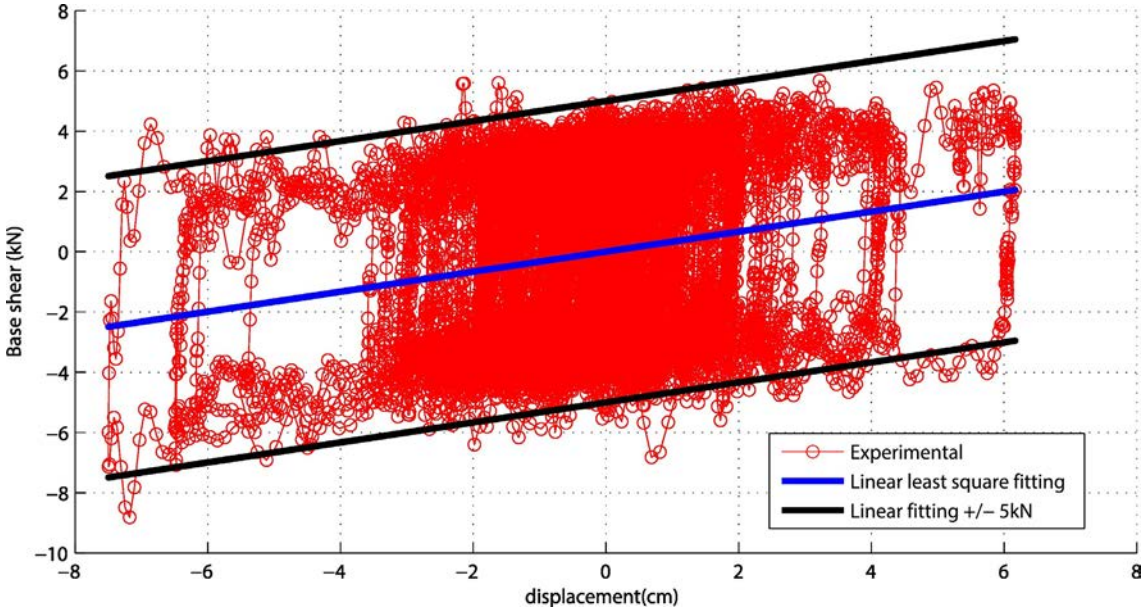

Fig. 16. Total base shear versus lateral tank displacement because of Hualañe accelerogram with a scale factor of 1.5 in the case CL.

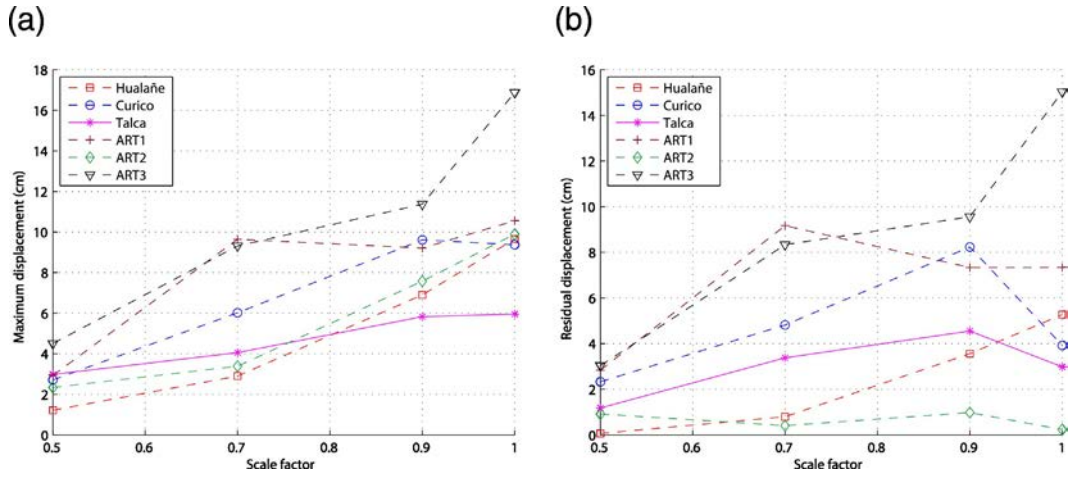

Fig. 17. (a) Maximum lateral displacement and (b) residual displacement of the tank versus scale factor for the six selected records in the case SB.

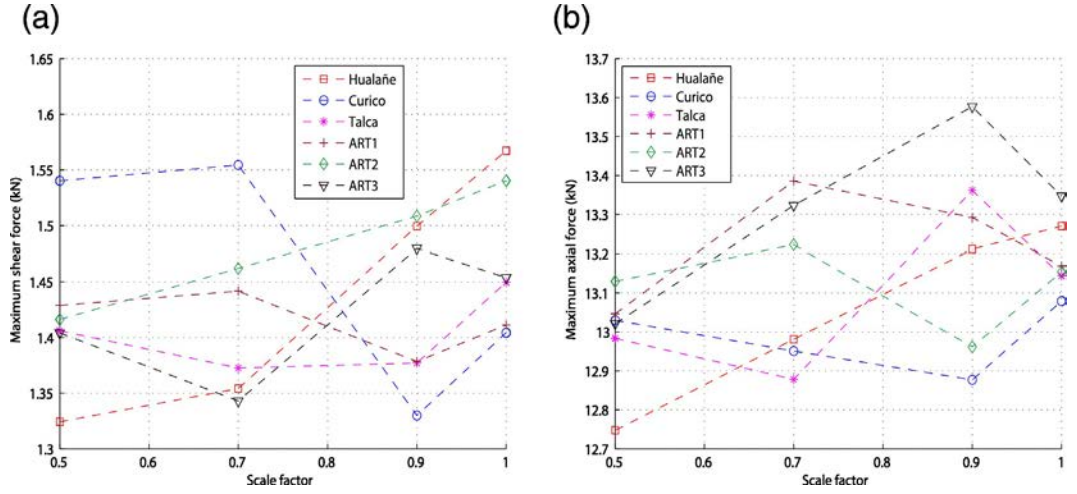

Fig. 18. Maximum values of (a) shear and (b) axial forces at the tank leg versus scale factor for the six selected records in the case SB.

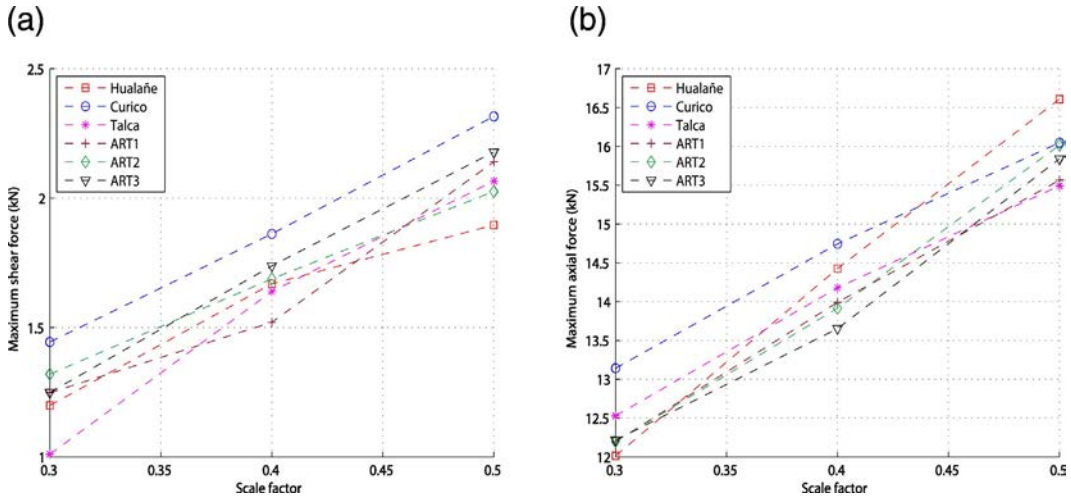

Fig. 19. Maximum values of (a) shear and (b) axial forces at the tank leg versus scale factor for the six selected records in the case FB.

would provoke failure at the piping connections and the surrounding structures. With respect to the residual displacement, Fig. 15(b) shows the residual displacement for each records and scale factors. The residual displacement varied from 1 cm and 3 cm, approximately, for a scale factor of 0.5, up to 15 cm, approximately, for a scale factor of 1. These results show that a restoring force is needed in order to guarantee lower residual displacements and to avoid failure of the piping connections and the surrounding structures.

Fig. 18(a) and (b) show the maximum values of the shear and axial forces at the tank leg, respectively. As explained above, the maximum shear and axial forces at the tank leg were bounded by the mobilized frictional force, and presented an average of 1.4 kN and 13.2 kN, respectively.

Finally, it is important to remark that, concerning the maximum shear and axial forces, no significant different were obtained between cases CL and SB. This was a consequence of the bound imposed by the mobilized frictional force, which value was very similar in both cases due to the flat sliding bearings were the same in both cases.

Table 2
Maximum responses of the legged wine storage tank for the three different analysed cases subjected to the six selected records.

Record	Case	Maximum values of				
		Used scale factor	Tank displacement (cm)	Residual tank displacement (cm)	Shear force at the tank leg (kN)	Axial force at the tank leg (kN)
Curicó	CL	1.5	7.7	0.7	1.61	12.71
	SB	1.0	9.4	3.9	1.15	13.08
	FB	0.5	–	–	2.32	16.05
Hualañe	CL	1.5	7.5	0.1	1.80	13.42
	SB	1.0	9.7	5.3	1.28	13.27
	FB	0.5	–	–	1.55	16.61
Talca	CL	1.5	8.1	0.1	1.49	12.97
	SB	1.0	6.0	3.0	1.19	13.14
	FB	0.5	–	–	2.07	15.49
ART1	CL	1.5	5.9	0.0	1.50	12.60
	SB	1.0	10.6	7.3	1.16	13.17
	FB	0.5	–	–	2.14	15.56
ART2	CL	1.5	5.4	0.1	1.50	12.60
	SB	1.0	9.9	0.2	1.26	13.15
	FB	0.5	–	–	2.03	16.02
ART3	CL	1.5	6.8	0.1	1.45	12.52
	SB	1.0	16.9	15.0	1.28	13.35
	FB	0.5	–	–	2.18	15.84

CL = tank with the multi-spring central leg and the flat sliding bearings. SB = tank with flat sliding bearings. FB = tank with fixed base.

6.3. Response of the fixed-base tank

The tank configuration with the fixed-base (case FB), i.e. fixed to the shaking table, was seismically tested using the previous described set of six records. The tests were conducted by scaling each record, starting from an intensity of 30% and repeating the test with increasing intensity up to 50%.

Fig. 19(a) and (b) show the maximum values of the shear and axial forces at the tank leg, respectively, for the used scale factors and records. In both figures, it can be observed that the trend is linear. The values of the maximum shear force varied from 1 kN and 1.2 kN, approximately, for a scale factor of 0.3, up to 1.6 kN and 1.9 kN, approximately, for a scale factor of 0.5. At the same time, the values of the maximum axial force varied from 12.5 kN and 13.5 kN, approximately, for a scale factor of 0.3, up to 15.5 kN and 16.5 kN, approximately, for a scale factor of 0.5.

It should be noted that higher values of scale factor were not used in this configuration (case FB) because the aim of this investigation was to compare the seismic intensity level required to reach a similar force demand on the tank leg for the three analysed cases, i.e. cases CL, SB and FB. In other words, in order to maintain the mock tank safety, the aim of this investigation was to obtain a similar force demand on the tank leg for the three analysed configurations, and compare the intensity level required to reach that demand and the lateral tank displacement.

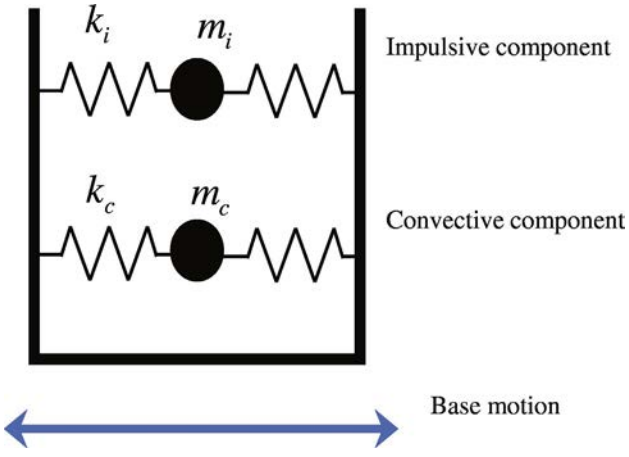

Fig. 20. Dynamic model typically used for liquid storage tanks.

6.4. Comparison between cases CL, SB and FB

A considerable increase in the capacity against failure of the structure was observed with the proposed seismic isolation system, i.e. case CL (see Table 2). For instance, in order for the tank with fixed-base configuration to reach a force demand on the tank leg similar to the one reached on cases CL and SB, a scale factor of 0.4 was necessary (see Fig. 19), which can be expressed as a PGA average of 0.17 g. On the other hand, for the tank with the isolation system with the multi-spring central leg and the flat sliding bearings, in order to reach a similar force demand on the tank leg, a scale factor of 1.5 was necessary, i.e. a PGA average of 0.63 g. As can be seen, a three time higher PGA was reached and no failure on the structure occurred. Therefore, comparing the PGA needed for a similar force demand on the tank leg in cases CL and FB, the reduction of the seismic demand on the tank leg in case CL was about 70%, compared to case FB. In other words, the force demand on the tank leg in case CL with a scale factor of 1.5 (PGA average = 0.63 g) was similar to the one in case FB with a scale factor of 0.4 (PGA average = 0.17 g).

For the tank with the flat sliding bearings and without the multi-spring central leg (case SB), the force demand on the tank leg was very similar to the one reached on case CL. However, as mentioned

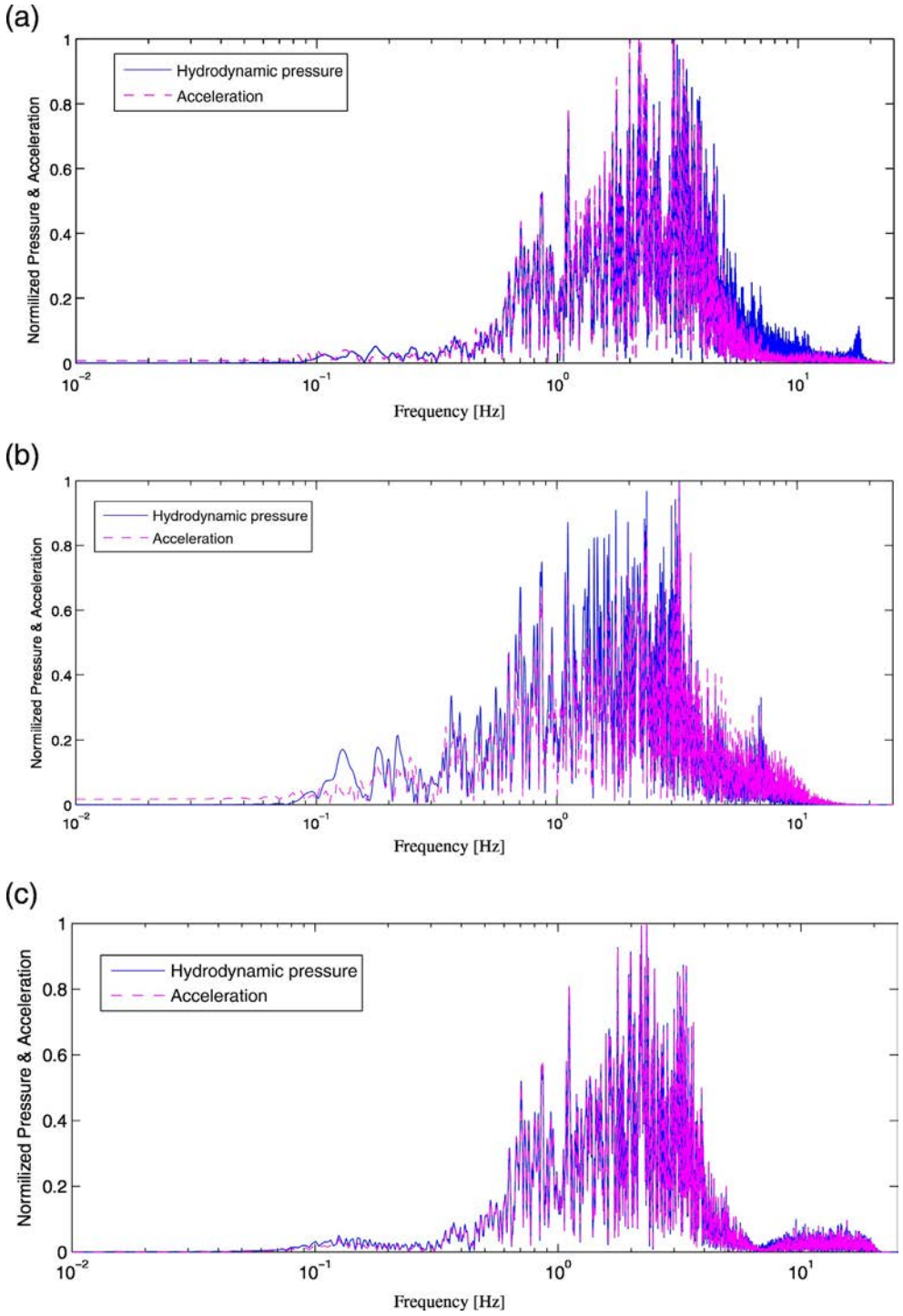

Fig. 21. Fourier transform of the hydrodynamic pressures and the accelerations for: (a) Hualañe accelerogram with a scale factor of 0.5 in case FB; (b) Hualañe accelerogram with a scale factor of 1.5 in case CL; and (c) Hualañe accelerogram with a scale factor of 1 in case SB.

above, the large displacements will provoke failures of the piping connections and the surrounding structures (see Table 2). For instance, the average of the maximum displacement for the six used records was 10.42 cm, for a scale factor of 1 in case SB (see Fig. 19). On the other hand, the average of the maximum displacement of case CL, and a scale factor 1.5, was 6.8 cm (see Fig. 13). This shows that even with an increase of 50% on the seismic intensity level (e.g. PGA), the maximum displacement of the tank was 34% less for case CL. Therefore, case SB would failure for a PGA of 0.42 g, while case CL would remain without failure for a PGA of 0.63 g.

This increase in the capacity against the failure of the tank in case CL was achieved due to 1) the bound on the maximum shear force transmitted to the tank by the effect of the mobilized frictional force, 2) the increase in the energy dissipated as a result of the friction at the bottom of the tank legs, 3) the changes on the period of the dynamic response of the structure and 4) the effectiveness of the multi-spring central leg acting as a restoring element.

6.5. Comparison between the hydrodynamic pressures and the accelerations

The main dynamic behaviour of liquid storage tanks are typically evaluated with a simplified mathematical model, which is shown in Fig. 20 [26,27]. The hydrodynamic pressures and forces in the tank can be expressed as the sum of two components. The first component is impulsive, representing the effect of the part of the liquid that moves in synchronism with the tank wall as a rigid body. The second component is convective, representing the effect of the part of the liquid that presents a sloshing motion. Each component has its respective mass and stiffness. However, as wine storage tanks are completely filled, sloshing was not possible. Therefore, the hydrodynamic pressures in the wine tank are caused only by the impulsive component.

In order to corroborate the above-mentioned conclusion, the hydrodynamic pressures and the accelerations at the bottom of the tank (see Fig. 12) were compared. The slenderness ratio of the considered tank was 2.1 (H_W/R). For brevity, the comparisons were carried out in the case FB for the Hualañe record with a scale factor of 0.5, in the case CL for the Hualañe record with a scale factor of 1.5, and in the case SB for the Hualañe record with a scale factor of 1. The hydrodynamic pressures and accelerations were normalized for the respective comparison in the frequency domain. As expected, the frequency content of both signals presented a good agreement (see Fig. 21). In other words, this comparison showed that the hydrodynamic pressures on the tank wall are in synchronism with the accelerations of the tank wall. Hence, the hydrodynamic pressures and forces in the complete wine-filled tank are caused only by the impulsive component.

Additionally, it is worth mentioning that the results herein presented can be extended for any of the above-mentioned options for realizing the restoring element (see Section 3). However, the deformation limits of these other options should be estimated. Ongoing researches are developing restoring elements made of rubber hinges, which work, principally, with their flexural stiffener.

7. Conclusions

Using a shaking-test campaign, the effectiveness of an isolation system design for the seismic protection of a typical legged wine storage tank was studied. The proposed isolation system is based on compression springs and flat sliding bearings. The tests have been performed using different experimental configurations: fixed base, isolated base with the multi-spring central leg and the flat sliding bearings, and isolated base only with the flat sliding bearings. During the tests, the tank has been subjected to six different accelerograms, which reproduce records of natural and artificial seismic events (3 natural and 3 artificial records). The results show the effectiveness of the proposed isolation system in reducing the maximum shear and axial forces at the tank legs. In particular, by focusing on the shear and axial forces at the tank legs and the lateral tank displacement, the following conclusions can be drawn:

- For legged wine storage tanks, this novel seismic isolation system can significantly reduce the seismic force demand on the tank legs.
- The use of just flat sliding bearings (without any restoring element) for seismic isolation of legged wine storage tanks provokes larger displacements of the tank, and these would provoke failure of the piping connections and the surrounding structures.
- The flexural, shear and axial stiffnesses of compression springs can be used to develop efficient restoring elements for the seismic isolation of legged wine storage tanks.
- The restoring force provided by the multi-spring central leg was effective in reducing the lateral tank displacement and the residual tank displacement. In particular, the maximum lateral displacement was reduced by 30%, even with an increase of 50% for the PGA.
- Using seismic isolation systems may represent a significant improvement in the seismic reliability of legged wine storage tanks

Acknowledgments

The authors wish to acknowledge the financial support provided by CONICYT-PCHA/Doctorado Nacional/2013-63130131 and the FONDECYT project number 1120937.

References

[1] D. Cooper, A history of steel tank structural design, Wine Business Monthly, 2004.
[2] E. González, J. Almazán, J. Beltrán, R. Herrera, V. Sandoval, Performance of stainless steel winery tanks during the 02/27/2010 Maule earthquake, Eng. Struct. 56 (2013) 1402–1418.
[3] G.C. Manos, Evaluation of the earthquake performance of anchored wine tanks during San Juan Argentina, 1977 earthquake, Earthq. Eng. Struct. Dyn. 20 (1991) 1099–1114.
[4] A. Niwa, R.W. Clough, Buckling of cylindrical liquid storage tanks under earthquake loading, Earthq. Eng. Struct. Dyn. 10 (1982) 107–122.
[5] G.C. Manos, R.W. Clough, Tank damage during May 1983 Coalinga earthquake, Earthq. Eng. Struct. Dyn. 1 (1985) 449–466.
[6] EERI Reconnaissance Team, Loma Prieta earthquake reconnaissance report, Earthquake Spectra 6 (1990) 189–238.
[7] EERI Reconnaissance Team, Preliminary observations on the December 22, 2003, San Simeon Earthquake, EERI Special Earthquake Report, 2004 (March).
[8] E.C. Fischer, J. Liu, A.H. Varma, Investigation of cylindrical steel tank damage at wineries during earthquakes: lessons learned and mitigation opportunities, Pract. Period. Struct. Des. Constr. (2016) (04016004).
[9] J.M. Kelly, Aseismic base isolation: review and bibliography, Soil Dyn. Earthq. Eng. 5 (4) (1986) 202–216.
[10] T.T. Soong, G.F. Dargush, Passive Energy Dissipation Systems in Structural Engineering, first ed. John Wiley & Sons, New York, 1997.
[11] M.K. Shrimali, R.S. Jangid, Seismic analysis of base-isolated liquid storage tanks, J. Sound Vib. 275 (2004) 59–75.
[12] K.H. Cho, M.K. Kim, Y.M. Lim, S.Y. Cho, Seismic response of base-isolated liquid storage tanks considering fluid–structure–soil interaction in time domain, Soil Dyn. Earthq. Eng. 24 (2004) 839–852.
[13] J.L. Almazán, F.A. Cerda, J.C. De la Llera, D. López-García, Linear isolation of stainless steel legged thin-walled tanks, Eng. Struct. 29 (7) (2007) 1596–1611.
[14] A. Maleki, M. Ziyaeifar, Damping enhancement of seismic isolated cylindrical liquid storage tanks using baffles, Eng. Struct. 29 (2007) 3227–3240.
[15] A. Maleki, M. Ziyaeifar, Sloshing damping in cylindrical liquid storage tanks with baffles, J. Sound Vib. 311 (2008) 372–385.
[16] M. Pirner, S. Urushadze, Liquid damper for suppressing horizontal and vertical motions—Parametric study, J. Wind Eng. Ind. Aerodyn. 95 (2007) 1329–1349.
[17] D. Liu, P. Lin, Three-dimensional liquid sloshing in a tank with baffles, Ocean Eng. 36 (2009) 202–212.
[18] P.K. Malhotra, Seismic strengthening of liquid-storage tanks with energy-dissipating anchors, J. Struct. Eng. 124 (4) (1998) 405–414.
[19] O. Curadelli, Seismic reliability of spherical containers retrofitted by means of energy dissipation devices, Eng. Struct. 33 (9) (2011) 2662–2667.
[20] M. Ormeño, M. Geddes, T. Larkin, N. Chouw, Experimental study of slip-friction connectors for controlling the maximum seismic demand on a liquid storage tank, Eng. Struct. 103 (2015) 134–146.
[21] J.I. Colombo, J.L. Almazán, Seismic reliability of continuously supported steel wine storage tanks retrofitted with energy dissipation devices, Eng. Struct. 98 (2015) 201–211.
[22] M.S. Chalhoub, J.M. Kelly, Theoretical and Experimental Studies of Cylindrical Water Tanks in Base Isolated Structures, Earthquake Engineering Research Center, University of California at Berkeley, 1988.

[23] F.F. Tajirian, Base isolation design for civil components and civil structures, Proceedings of the Structural Engineers World Congress, San Francisco, CA Jul 18 1998, pp. 233–244.
[24] M. De Angelis, R. Giannini, F. Paolacci, Experimental investigation on the seismic response of a steel liquid storage tank equipped with floating roof by shaking table tests, Earthq. Eng. Struct. Dyn. 39 (4) (2010) 377–396.
[25] NCH INN, NCh 2369.Of 2003. Earthquake Resistant Design of Industrial Structures and Facilities, Instituto Nacional de Normalización, Santiago, Chile, 2003.
[26] A.S. Veletsos, Y. Tang, Soil-structure interaction effects for laterally excited liquid storage tanks, Earthq. Eng. Struct. Dyn. 4 (1990) 473–496.
[27] A.S. Veletsos, P. Shivakumar, Y. Tang, H.T. Tang, Seismic response of anchored steel tanks, in: A.J. Gupta (Ed.), Proc, 3rd Symposium on Current Issues Related to Nuclear Power Plant Struct., Equip., and Piping, North Caroline State Univ., N.C. 1990, pp. 2–15.